International Journal of Trend in Scientific Research and Development (IJTSRD)
Volume 10 Issue 6, Nov-Dec 2026 Available Online: www.ijtsrd.com e-ISSN: 2456 – 6470

Exploring Potential Inhibitors of Serine/Threonine-Protein Kinase N1 through Virtual Screening and Molecular Dynamics Simulation Studies

Mohammad Amaan Khan[1], Arunabh Choudhury[2], Dr. Md Imtaiyaz Hassan[3]

[1]PG Scholar, [2]Research Scholar, [3]Professor,
[1]Department of Computer Science, Faculty of Natural Sciences, Jamia Millia Islamia, Delhi, India
[2,3]Centre for Interdisciplinary Research in Basic Sciences, Jamia Millia Islamia, Delhi, India

ABSTRACT

Protein kinase N1 (PKN1) is a Ser/ Thr kinase that phosphorylates tau at multiple sites within its microtubule binding repeats. Under normal conditions, PKN1-mediated phosphorylation regulates tau dynamics and supports microtubule stability. PKN1 activity becomes dysregulated in tauopathies, driving tau into a hyperphosphorylated state. Hyperphosphorylated tau detaches from microtubules, misfolds, and oligomerizes into toxic aggregates that disrupt axonal transport and synaptic communication. These aggregates seed the formation of neurofibrillary tangles and contribute to neuronal dysfunction and death. Elevated PKN1 expression and activity have been observed in the brains of patients with frontotemporal dementia and Alzheimer's disease (AD), indicating its central role in tau-driven neurodegeneration. In this study, we employed an integrated virtual screening approach of molecular docking and molecular dynamics (MD) simulations to identify phytochemical inhibitors of PKN1 from the IMPPAT database. Molecular docking screening via InstaDock identified the top 50 hits with string binding affinities (−11.9 kcal/mol to−11.1 kcal/mol) to PKN1. Subsequent ADMET and PASS analyses filtered out compounds with favorable pharmacokinetic profiles. Interaction analysis using Discovery Studio Visualizer and PyMOL further elucidated binding conformations of selected compounds with PKN1. Top hits underwent 100 ns MD simulations using GROMACS to validate the stability of the interactions. Finally, we propose two phytochemicals, IMPHY012968 and IMPHY009264, with appreciable drug-likeliness and binding potential with PKN1. The current study identifies IMPHY012968 and IMPHY009264 as promising PKN1 inhibitors, highlighting their therapeutic potential for Alzheimer's disease (AD) and warranting further validation.

How to cite this paper: Mohammad Amaan Khan | Arunabh Choudhury | Dr. Md Imtaiyaz Hassan "Exploring Potential Inhibitors of Serine/Threonine-Protein Kinase N1 through Virtual Screening and Molecular Dynamics Simulation Studies" Published in International Journal of Trend in Scientific Research and Development (ijtsrd), ISSN: 2456-6470, Volume-10 | Issue-6, December 2026, pp.30-41, URL: www.ijtsrd.com/papers/ijtsrd150296.pdf

IJTSRD150296

Copyright © 2026 by author (s) and International Journal of Trend in Scientific Research and Development Journal. This is an Open Access article distributed under the terms of the Creative Commons Attribution License (CC BY 4.0) (http://creativecommons.org/licenses/by/4.0)

KEYWORDS: *Protein kinase N1, Alzheimer's disease, IMPPAT database, phytochemicals, MD simulations.*

INTRODUCTION

Protein kinase N1 (PKN1) is a serine/threonine kinase belonging to the protein kinase C (PKC) superfamily and the AGC kinase group. It serves as a multifunctional signaling effector that integrates upstream cues to regulate cytoskeletal organization, cell survival, migration, proliferation, apoptosis, and adaptive stress responses. PKN1 is activated primarily downstream of Rho family GTPases, particularly RhoA and Rac1, and is also influenced by lipid-derived second messengers. Through these inputs, PKN1 participates in a broad range of intracellular signaling networks relevant to normal physiology as well as disease progression. Owing to these diverse functions, PKN1 has attracted considerable interest in cancer biology, neurobiology, neurodegenerative disorders, and metabolic regulation[1,2,3-5].

Structurally, PKN1 consists of an N-terminal regulatory region and a C-terminal catalytic kinase domain. The regulatory segment contains three homologous region-1 (HR1) motifs that mediate interactions with active Rho GTPases and contribute to localization-dependent kinase activation. In addition, a C2-like domain supports membrane

association through lipid interactions. The catalytic region contains conserved motifs required for ATP binding, substrate recognition, and phosphotransferase activity. Activation of PKN1 is generally achieved through conformational rearrangement induced by Rho GTPase binding, accompanied by phosphorylation-dependent stimulation of the kinase domain[6,7,8,9-14].

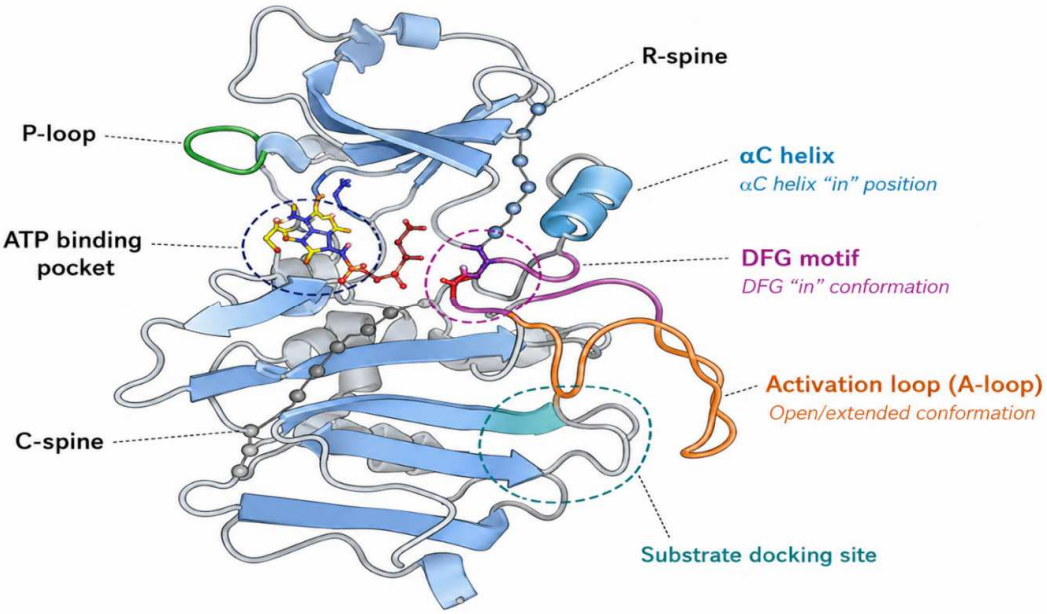


Figure 1. Structural organization of the PKN1 kinase domain, highlighting key catalytic elements including the ATP-binding pocket, P-loop, αC helix, DFG motif, activation loop, and substrate docking region.

PKN1 is broadly expressed in mammalian tissues, with particularly prominent expression in the nervous system, where it contributes to neuronal integrity and cytoskeletal homeostasis. In neurons, PKN1 regulates neurofilament assembly and axonal transport, both of which are essential for maintaining axonal architecture and efficient neuronal communication. Dysregulation of PKN1 signaling has been associated with abnormal neurofilament accumulation and impaired axonal trafficking, pathological features commonly observed in neurodegenerative disorders such as amyotrophic lateral sclerosis (ALS). These findings indicate that PKN1-mediated phosphorylation of neuronal substrates is critical for preserving neuronal homeostasis. Beyond the nervous system, PKN1 participates in several signaling pathways that control cellular growth and metabolism. It has been implicated in phosphoinositide signaling, PKC-related cascades, AKT signaling, and Wnt/β-catenin pathways. In melanoma models, PKN1 negatively modulates canonical Wnt signaling by limiting WNT3A-induced phosphorylation of the LRP6 co-receptor. PKN1 also phosphorylates TRAF1, thereby influencing tumor necrosis factor receptor–dependent survival signaling. In adipocytes, PKN1 has been shown to support insulin-stimulated GLUT4 translocation and glucose uptake, suggesting an important role in metabolic regulation and insulin responsiveness[15-21,22,23].

Recent studies have further emphasized the role of PKN1 in neuronal development and synaptic organization. PKN1 regulates the activity of the transcription factor NeuroD2 in the hippocampus and cerebellum, at least in part through modulation of AKT signaling. Loss of PKN1 function has been linked to excessive AKT activation, aberrant synaptogenesis, neuronal degeneration, and motor dysfunction. Since NeuroD2 dysregulation has been implicated in neurodevelopmental and psychiatric conditions, including epilepsy, autism spectrum disorder, schizophrenia, and depression, PKN1 is increasingly recognized as an important regulator of neuronal maturation and brain circuit formation. PKN1 has also emerged as a molecule of interest in oncology. Elevated expression or activation of PKN1 has been reported in several malignancies, including prostate, ovarian, melanoma, hepatocellular, and endometrial cancers. In prostate cancer, PKN1 enhances androgen receptor–dependent transcription and promotes invasive phenotypes. In endometrial carcinoma, PKN1 contributes to transforming growth factor-β (TGF-β) and epidermal growth factor (EGF)-mediated signaling pathways that favor proliferation and metastatic progression. These observations support the potential utility of PKN1 as both a prognostic biomarker and a therapeutic target in selected tumor types[24,25,26,27-33].

Emerging evidence also suggests a role for PKN1 in metabolic stress and ischemic injury. PKN1 negatively regulates phosphoglucomutase 2-like 1 (PGM2L1), a protein involved in glucose metabolism and mitochondrial

pyruvate utilization in neurons. Experimental studies in PKN1-deficient models have demonstrated altered cerebral glucose handling and modified responses to ischemic insult. Notably, reduced PKN1 activity has been associated with attenuated inflammatory responses and decreased tissue damage during ischemia-reperfusion injury, indicating a potential role in neurovascular stress adaptation[34-36].

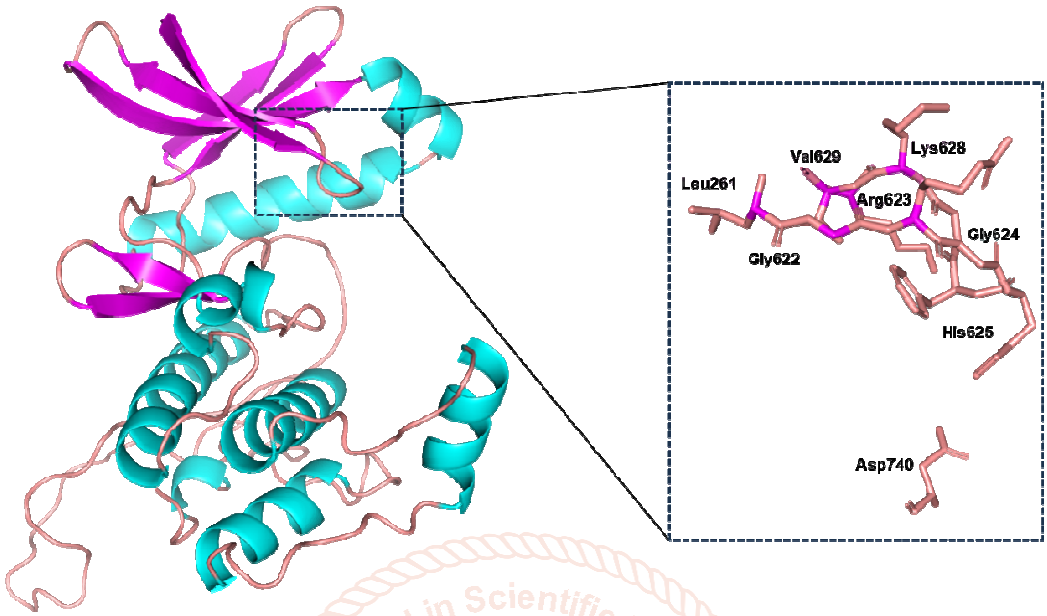


Figure 2. Three-dimensional representation of PKN1 structure showing the organization of α-helices, β-sheets, and residues contributing to substrate interaction within the catalytic core.

Overall, PKN1 functions as a multifunctional signaling kinase that integrates inputs from Rho GTPases, membrane lipids, and growth-related pathways to regulate cytoskeletal dynamics, neuronal differentiation, metabolic homeostasis, and tumor progression [1,15,21-23,29-35]. By coordinating multiple intracellular signaling networks, PKN1 contributes to the maintenance of cellular homeostasis under physiological and pathological conditions [15-18,21,22,23-28,34-36]. Given its involvement in neurodegeneration, cancer, and metabolic dysfunction, PKN1 continues to emerge as a promising target for future translational and therapeutic research [16-18,29-31,34-36].

MATERIALS & METHODS

Web and Computational Resources

To perform this study, a highly protective HP workstation with a 1.19 GHz CPU and 8 GB RAM running a 64-bit Windows operating system was used. All the superpower facilities and fast internet connectivity without any disturbance were utilized. In this experiment, several online servers were utilized for analysis and data retrieval, such as UniProt, RCSB PDB, PubMed, SwissADME, PASS online server, pKCSM, IMPPAT database (http://cb.imsc.res.in/imppat/) and a Library prepared from existing inhibitors of PKN1(PubMed). Additionally, various bioinformatics standalone software were used like PyMOL, Discovery Studio Visualizer, InstaDock, QtGrace (Boreak 2021).

Receptor and Ligand Preparation

The suitable PKN1 structure is selected and retrieved using UniProt (Consortium 2019) and PDB, based on high resolution, existence of kinase domain, mutation sequence, ligand associated, and purity of structure. The X-ray crystal structure of human PKN1 (PDB ID:4OTH, Resolution: 1.80 Å) was obtained in PDB format from the RCSB website (http://www.rcsb.org) and improved further using PyMOL by eliminating water molecules, heteroatoms and co-crystal ligands to obtain a native structure. The protein was visualised using PyMOL and it is found that there is no break or missing residues, so pre-processing was not required.

Database for Screening

In structural biology, molecular docking is a frequently used approach for predicting the best binding conformation of a receptor-ligand interaction. One of the essential aspects to consider when developing a compound library for an effective virtual screening strategy is to provide a database with the most structural variety possible. This enhances the likelihood of discovering an acceptable hit. Drug Bank (Wishart, Feunang et al. 2018), PubChem, and IMPPAT database are only a few of the open access for small molecule libraries.

Whereas the corporate databases of big pharmaceutical corporations maintain a few million compounds. IMPPAT is a manually curated database of 4010 Indian medicinal plants consisting of 17967 phytochemicals having 1095 therapeutic uses. We created a plant based natural compounds library with 17,967 compounds from IMPPAT database [37] for VS process.

Input Files and Directories

InstaDock, an open-source Windows-based GUI software that performs molecular docking-based virtual screening and automated continuous docking of vast chemical databases against protein kinase, was employed in our study. InstaDock uses OpenBabel and Rasmol internally to handle file conversion and visualization responsibilities, respectively. This creates a 'Result' folder in which all docked files, docking scores, top hits, and their split conformers are saved as a spreadsheet and text files. To perform molecular docking, a working directory containing InstaDock, the receptor.pdb file, and the ligand files must be generated. When you execute the application, it converts the ligand's PDB files to the PDBQT format required for docking. InstaDock also generates a configuration file for grid preparation. This sets the 3D range in which all ligands should dock. In addition to docking, we retrieved the top 50 hits in an Excel document based on their docking score, binding affinity, and many other files separately from the respective libraries.

Virtual Screening Methodology

The receptor-ligand docking method is used for ligand screening against the PKN1 X-ray crystal structure (PDB ID: 4OTH). Molecular docking is an essential tool for establishing ligands' orientation within a receptor's active site cavity to understand the substrate inhibitor selectivity process. The ligands were obtained in PDBQT format from the IMPPAT database, and the library prepared was from similar structures of the existing PKN1 inhibitors, which include a natural chemical library. The bonding conformations and binding affinity of ligands with the kinase create the analytical foundation of molecular docking. During docking, energy grid boxes supply ligands with a specific docking area, ensuring optimal binding affinity and structural pose of ligand-protein complexes within space. InstaDock defines the dimensions grid box centre x, y, z along with size parameter values x, y, z as -22.577, -1.512, -15.445; and 71, 72, 64, accordingly. Several ligand orientations in the active site cavity of the receptor are explored using the docking technique. Each time it docks a ligand, it provides a random seed and scoring function, which is the foundation for the ligand's binding affinity towards protein [90].

InstaDock assessed the docking outcomes from log files and out files once the screening completed, afterwards, the optimum docked conformation was opted for further investigation. The visualization and structural analysis of docked complexes was completed with PyMOL and Discovery Studio Visualizer. On the filtered compounds, we ran SwissADME server (http://www.swissadme.ch/) to detect PAIN (Loeser and Melzack 1999), pkCSM (http://biosig.unimelb.edu.au/pkcsm) to investigate physicochemical properties, ADMET properties (absorption, distribution, metabolism, excretion, toxicity), and lastly, way-2-drug to evaluate the pharmacological properties ligands- receptor interaction with activation probability (Pa) greater than 0.3.

MD Simulation

The virtual screening discoveries led to a molecular mechanics level, where we conducted 100 ns MD simulations on four finalized compounds from each library at 300 K on the GROMACS simulation suite under the Gromos force field. Topologies and force field parameters were developed for each compound via CgenFF. Each ligand-PKN1 system was simulated in a virtual cubic box of water with a dimension of 10 Å and solvated using the gmx solvate module in the Simple Point Charge (SPC) water model. Additionally, all systems were energy-minimized using a 1500-step steepest descent algorithm, followed by charge neutralization. The temperature of all systems was adjusted from 0 to 300 K over a 1000-ps equilibration phase at constant volume under periodic boundary conditions. Quality check metrics such as kinetic energy, volume, density, and enthalpy were used to authenticate the obtained simulations for PKN1 and its ligand complexes. The simulated GROMACS trajectories were generated on parameters including RMSD, RMSF, Rg, SASA, PCA, and others, for each residue with respect to time function, wherein QtGrace plotted graphs and figures to illustrate PKN1 residual interaction and stability on ligand binding.

RESULTS & DISCUSSION

PKN1, is a protein Ser/Thr kinase that converts extracellular stimuli into a wide range of responses. Multiple pathways of PKN1, including coordinated regulation of gene expression, metabolism, motility, survival, apoptosis, and differentiation. A detailed virtual screening and MD simulations procedure of PKN1 with IMPPAT-based plant compounds is discussed in the following sections.

1. Libraries of drug-like compounds

IMPPAT database prepared from a similar structure of existing inhibitors of PKN1 of 17,967 and 6,000 phytochemical and bioactive natural substances on virtual screening, molecular docking, and MD simulation was successfully achieved. The IMPPAT database holds 17,967 phytochemicals, of which 11,708 and 2649 compounds from each library were consolidated in a library based on pharmacological similarities as per the Lipinski rule of five. The Lipinski rule of five is a fundamental parameter as well as a threshold value for a chemical substance to act as a therapeutic, wherein the molecular weight, hydrogen bond donor, hydrogen bond acceptor, logS, and logP value should be less than 500, 5, 10 and 5 respectively and das the compounds that violated any of the previously mentioned criteria were excluded for further process.

2. Docking-based Virtual Screening

A comprehensive strategy of virtual screening of ligands was undertaken to discover PKN1 selective inhibitors. As a conclusion, the docking software created log files and output files for each compound, which included affinity scores and docked poses, respectively, which were then employed to eliminate compounds based on unsuitable binding affinities, docking score, and binding position. The VS delivered many phytochemicals and bioactive compounds with high binding affinity towards the PKN1 binding cavity, making them viable candidates for additional screening in investigating potential PKN1 inhibitors. The filtering of docked output revealed 50 hits out of 11,708 compounds, respectively, with a significant binding affinity to PKN1, ranging from –11.9 to –11.1 kcal/mol. Since a higher negative binding affinity value indicates a more stable receptor-ligand complex, we anticipate stable complexes on PKN1 binding to 50 hits from each library.

Table 1: Binding of top 50 hits produced by InstaDock from IMPPAT

S. No.	Compound ID	Binding Free Energy (kcal/mol)	p*Ki*	Ligand Efficiency (kcal/mol/non-H atom)	Torsional Energy
1.	IMPHY010691	-11.9	8.73	0.3306	0.9339
2.	IMPHY012275	-11.8	8.65	0.3806	0.3113
3.	IMPHY007015	-11.8	8.65	0.3806	0.6226
4.	IMPHY009308	-11.7	8.58	0.3774	0.6226
5.	IMPHY010508	-11.7	8.58	0.3774	0.6226
6.	IMPHY006882	-11.6	8.51	0.4143	0
7.	IMPHY009264	-11.6	8.51	0.3625	0.3113
8.	IMPHY002477	-11.6	8.51	0.3515	0.6226
9.	IMPHY010403	-11.6	8.51	0.3742	0.6226
10.	IMPHY013217	-11.6	8.51	0.3742	1.2452
11.	IMPHY001575	-11.5	8.43	0.371	0.3113
12.	IMPHY010181	-11.5	8.43	0.3594	0.3113
13.	IMPHY010395	-11.5	8.43	0.371	0.6226
14.	IMPHY013142	-11.5	8.43	0.3966	0.6226
15.	IMPHY013522	-11.5	8.43	0.3382	1.5565
16.	IMPHY004577	-11.4	8.36	0.456	0.3113
17.	IMPHY011162	-11.4	8.36	0.3677	0.3113
18.	IMPHY013714	-11.4	8.36	0.3455	0.3113
19.	IMPHY001137	-11.3	8.29	0.452	0
20.	IMPHY001305	-11.3	8.29	0.4346	0
21.	IMPHY002674	-11.3	8.29	0.452	0
22.	IMPHY000366	-11.3	8.29	0.3645	0.3113
23.	IMPHY001734	-11.3	8.29	0.3645	0.3113
24.	IMPHY005266	-11.3	8.29	0.3767	0.6226
25.	IMPHY009120	-11.3	8.29	0.3424	0.6226
26.	IMPHY010369	-11.3	8.29	0.3767	0.6226
27.	IMPHY010851	-11.3	8.29	0.3645	0.6226
28.	IMPHY014734	-11.3	8.29	0.3645	0.6226
29.	IMPHY013216	-11.3	8.29	0.3645	1.2452
30.	IMPHY004031	-11.2	8.21	0.487	0
31.	IMPHY009331	-11.2	8.21	0.4308	0

32.	IMPHY012968	-11.2	8.21	0.4	0
33.	IMPHY002449	-11.2	8.21	0.4	0.3113
34.	IMPHY000290	-11.2	8.21	0.4148	0.6226
35.	IMPHY008760	-11.2	8.21	0.3613	0.6226
36.	IMPHY014742	-11.2	8.21	0.3613	0.6226
37.	IMPHY009548	-11.2	8.21	0.3294	0.9339
38.	IMPHY010989	-11.2	8.21	0.3294	1.2452
39.	IMPHY003563	-11.2	8.21	0.3613	1.8678
40.	IMPHY004539	-11.1	8.14	0.444	0
41.	IMPHY006688	-11.1	8.14	0.4625	0
42.	IMPHY002578	-11.1	8.14	0.444	0.3113
43.	IMPHY003806	-11.1	8.14	0.3964	0.3113
44.	IMPHY005775	-11.1	8.14	0.3581	0.3113
45.	IMPHY007613	-11.1	8.14	0.3265	0.3113
46.	IMPHY008874	-11.1	8.14	0.4269	0.3113
47.	IMPHY004234	-11.1	8.14	0.3581	0.6226
48.	IMPHY004515	-11.1	8.14	0.3964	0.6226
49.	IMPHY007489	-11.1	8.14	0.4269	0.6226
50.	IMPHY013253	-11.1	8.14	0.3828	0.6226

3. ADMET Property Analysis

The ADMET properties of the top 50, namely Absorption, Distribution, Metabolism, Excretion, and Toxicity, were comprehensively studied to understand the key Chemical nature of chosen compounds that let substances establish as potent PKN1 inhibitors. This procedure made use of the pkCSM webserver, and compounds are anticipated to have excellent ADMET properties. Furthermore, using SwissADME, the PAINS (Pan-Assay Inference compound structure) were investigated, and no chemical possessed such PAINS Inside its structure.

Table 2: ADMET properties of top 6 hits of PKN1.

S. No.	Compound	GI absorption	Ali Class	BBB permeant	CYP2D6 inhibitor	Hepatotoxicity	AMES toxicity
1.	IMPHY012968	High	Moderately soluble	Yes	No	No	No
2.	IMPHY010369	High	Moderately soluble	Yes	Yes	Yes	No
3.	IMPHY002578	High	Moderately soluble	Yes	No	Yes	Yes
4.	IMPHY004577	High	Moderately soluble	Yes	No	Yes	Yes
5.	IMPHY009120	High	Moderately soluble	Yes	No	No	No
6.	IMPHY009264	High	Moderately soluble	Yes	No	No	No

4. PASS Analysis

Furthermore, the Way2Drug online server performed a PASS analysis on all selected compounds to predict biological activity, i.e., anti-cancer activities, to provide potential therapeutic leads for PKN1-mediated cancer. As a result, the server predicted two compounds. These compounds are projected to have antineoplastic and kinase inhibitory activities as they own high Pa values (Pa> 0.3 when Pa values are greater than Pi).

Table 3: Selected compounds and their biological properties

S. No.	Compounds	Pa	Pi	Activity
1.	**IMPHY012968**	0,810	0,010	Antineoplastic
		0,478	0,008	Antioxidant
		0,476	0,040	Kinase inhibitor
		0,323	0,141	Anti-inflammatory

2.	**IMPHY009264**	0,917	0,005	Antineoplastic
		0,683	0,018	Anti-inflammatory
		0,612	0,004	Dementia treatment
		0,650	0,056	Nootropic

A. Interaction analysis

Discovery Studio Visualizer was used to generate two-dimensional interaction diagrams for PKN1 with the two selected compounds IMPHY012968 and IMPHY009264 (**Figure 3**). Following PASS analysis, PyMOL confirmed each ligand's docking conformations and binding patterns within the PKN1 binding cavity. The docking study produced nine poses for each compound, allowing for a detailed comparison of their binding interactions.

Figure 4A shows that IMPHY012968 formed stabilizing interactions such as hydrogen bonds. Additional van der Waals contacts with hydrophobic residues further secured the ligand within the PKN1 pocket. **Figure 4B** illustrates the binding of IMPHY009264. This compound also interacts with the binding site residues of PKN1, indicating deep insertion into the binding site and suggesting a strong inhibitory potential.

Both IMPHY012968 and IMPHY009264 show strong affinity for residues in the binding site and catalytic core, suggesting that they may effectively block ATP access and modulate PKN1 function. Given PKN1's role in neuroinflammation and tau hyperphosphorylation in AD, these compounds are promising for further development in targeting neurodegenerative pathways.

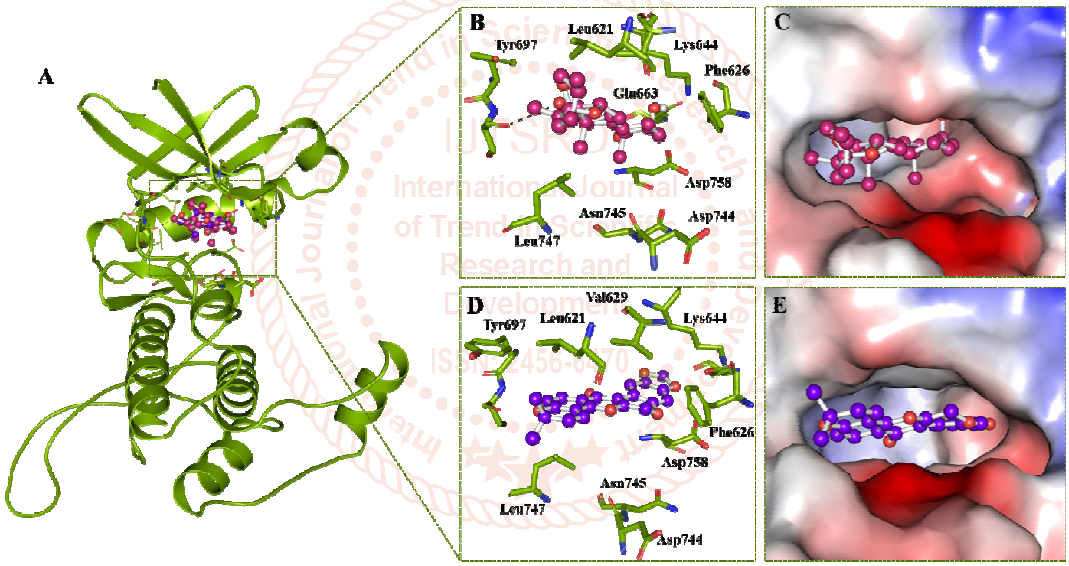


Figure 3: Binding site interaction of PKN1 with IMPHY012968 and IMPHY009264 as shown in ball and stick representation in pink and violet colors, respectively.

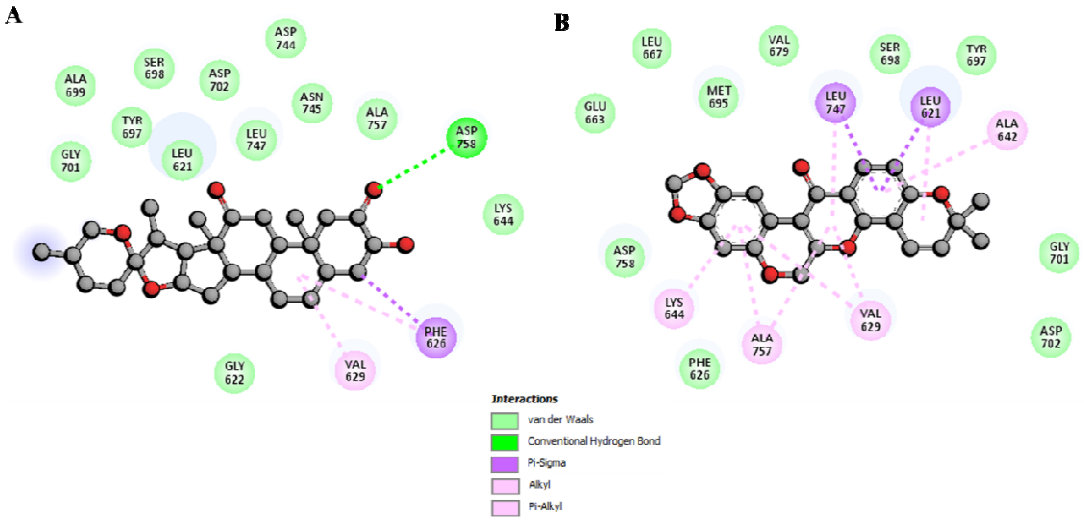


Figure 4: The two-dimensional interaction plots of PKN1 with (A) IMPHY012968, (B) IMPHY009264.

B. MD simulations

We performed a 100 ns MD simulation to evaluate PKN1 stability and structural dynamics in its free and complex forms. The docked conformations of each ligand were used in the solvent-based MD simulations. The free PKN1 and PKN1-ligand complexes (PKN1-IMPHY012968, PKN1-IMPHY009264) were subjected to 100 ns MD simulations using the initial orientations retrieved from molecular docking as starting structures. During the simulations, key structural parameters were observed to investigate how ligand binding affects the flexibility and conformational behaviour of proteins over time.

Table 4: Average values of RMSD, RMSF, *R*g, SASA and intramolecular

System	RMSD (nm)	RMSF (nm)	*R*g (nm)	SASA (nm^2)	#H-bonds
PKN1	0.72	0.22	2.04	161.38	152
PKN1-IMPHY009264	0.84	0.25	2.14	168.08	154
PKN1-IMPHY012968	0.71	0.26	2.08	164.17	151

I. Structural deviations

The root mean square deviation (RMSD) analysis evaluated the structural deviation for native PKN1 and PKN1-ligand complexes. The average RMSD values for PKN1 (PKN1-IMPHY012968, PKN1-IMPHY009264 complex were 0.72 nm, 0.84 nm, and 0.71 nm, respectively, over the 100 ns simulations (**Figure 5A**). These findings indicate that IMPHY012968 and IMPHY009264 stabilized PKN1 in a bound state, while PKN1 after binding to a control showed some atomic deviation from the mean binding position. Among the complexes, PKN1-IMPHY009264 showed the most consistent and stable RMSD trajectory, similar to the unbound protein. In contrast, the PKN1-IMPHY012968 complex showed increased deviations throughout the trajectory, indicating less favourable binding interactions. Overall, these results support the structural compatibility and stabilizing effect of the IMPPAT-based compounds on PKN1, particularly IMPHY009264, and highlight its potential as a lead candidate for AD treatment.

To evaluate residue-level flexibility in PKN1 and its ligand-bound forms, root mean square fluctuation (RMSF) analysis was performed for each system over a 100-ns MD simulation. RMSF provides insight into how individual amino acid residues deviate from their average positions over time, revealing local flexibility and dynamic behaviour in the protein structure. The average RMSF values observed for free PKN1, PKN1-IMPHY012968, and PKN1-IMPHY009264 complexes were 0.22 nm, 0.25 nm, and 0.26 nm, respectively (**Figure 5B**). These results indicate that the binding of IMPHY012968 had minimal effect on the protein's residue flexibility, showing nearly identical fluctuations to the free PKN1. Similarly, PKN1–IMPHY009264 exhibited a consistent fluctuation pattern but with a slightly higher average RMSF, suggesting mild localized flexibility. All complexes exhibited relatively uniform RMSF profiles, with occasional peaks. However, the IMPPAT-based ligands, particularly IMPHY009264, maintained consistent stability across most residue regions.

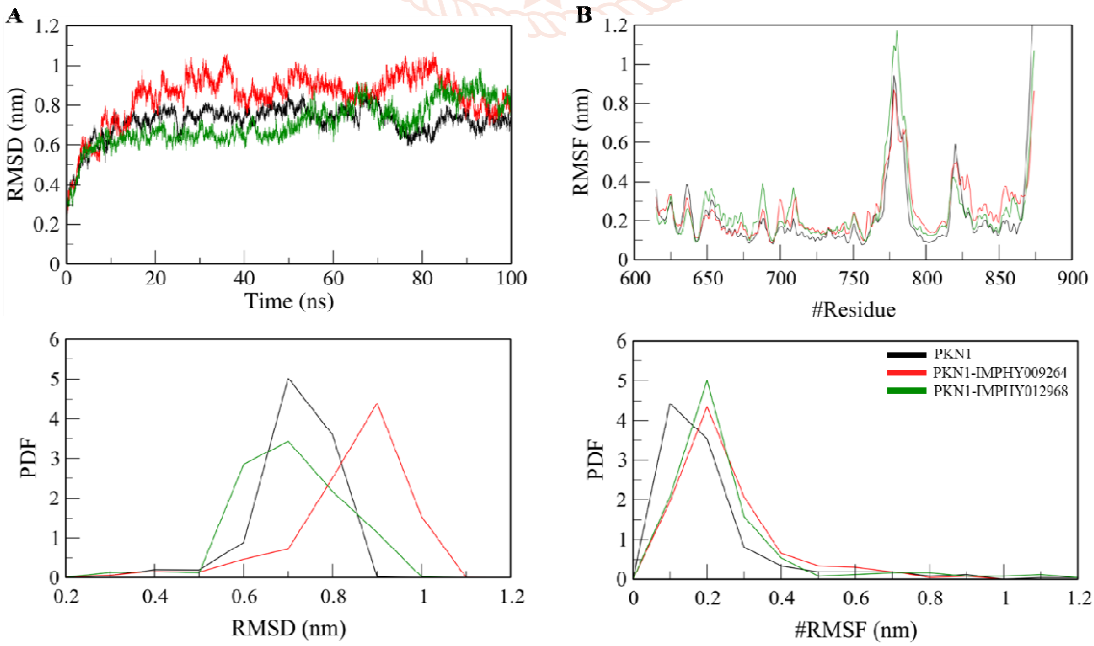


Figure 5: The (A) RMSD, (B) RMSF plot of PKN1 in its free form and complex form with IMPHY012968 and IMPHY009264. The lower panels show the probability density function (PDF).

II. Structural compactness

The radius of gyration (*R*g) was calculated for each 100 ns MD trajectory to assess the global compactness of PKN1 in the four systems. *R*g measures the root-mean-square distance of the protein's atoms from its center of mass, with lower values indicating a more tightly folded (and typically more stable) conformation. The average *R*g values were 2.04 nm for both unbound (apo) PKN1, 2.14 nm for the PKN1-IMPHY012968 complex, and 2.08 nm for the PKN1-IMPHY009264 complex (**Figure 6A**).

The solvent-accessible surface area (SASA) was calculated over the 100 ns MD trajectories to evaluate how ligand binding influences the exposure of PKN1's surface to solvent. SASA measures the total area of the protein that is accessible to water molecules, with lower values indicating a more buried, compact structure and higher values reflecting increased surface exposure. The average SASA values were 161.38 nm² for unbound PKN1, 168.08 nm² for PKN1-IMPHY012968, 164.17 nm² for PKN1-IMPHY009264 (**Figure 6B**). These closely clustered values demonstrate that all systems maintained a similar degree of solvent exposure throughout the simulations. Notably, PKN1-IMPHY009264 exhibited only a marginal increase in SASA (164.17 nm²) relative to the apo protein (161.38 nm²), suggesting that binding of this zinc-based ligand does not substantially disturb the protein's overall folding or packing. Overall, the minimal variations in SASA across the four systems together with consistent *R*g results underscore the structural integrity of PKN1 and its complexes, confirming that ligand binding preserves global compactness while allowing necessary surface flexibility.

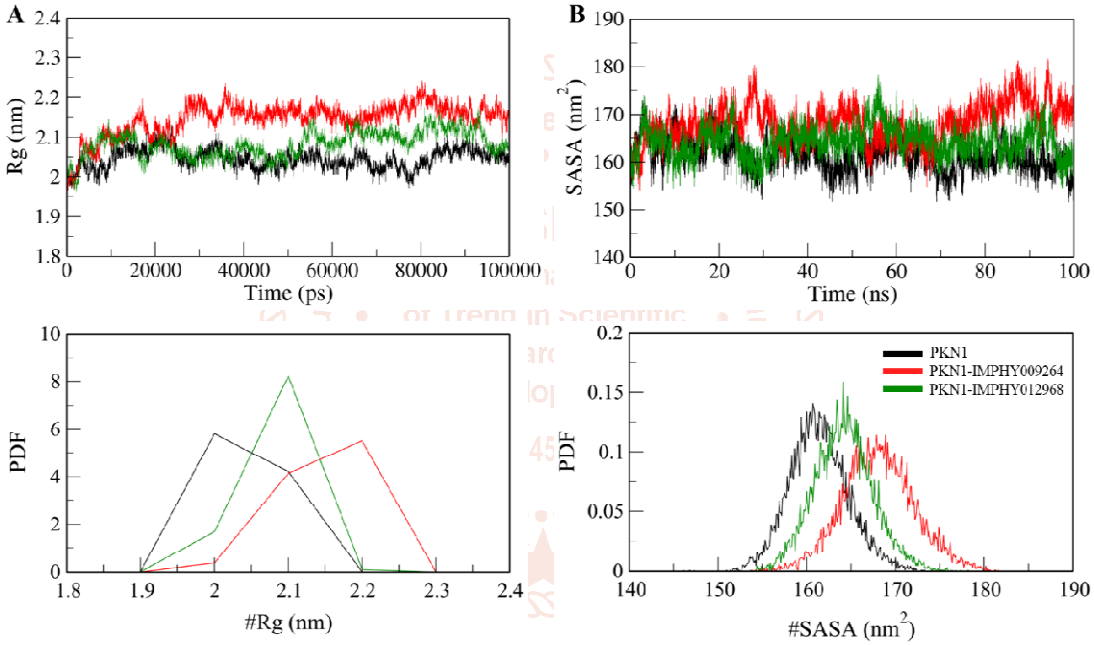


Figure 6: The (A) *R*g, (B) SASA plot of PKN1 in its free form and complex form with IMPHY012968 and IMPHY009264. The lower panels show the probability density function (PDF).

III. Dynamics of Hydrogen bonds

Intramolecular hydrogen bonds were analysed over the 100 ns MD trajectories to evaluate how ligand binding influences PKN1's internal stability and folding dynamics. Intramolecular hydrogen bonds, formed between donor and acceptor atoms within the protein backbone and side chains that serve as key stabilizing interactions that maintain secondary and tertiary structure. The average counts of intramolecular hydrogen bonds were 152 for unbound PKN1, 154 for the PKN1-IMPHY012968 complex, and 151 for PKN1–IMPHY009264 complex (**Figure 7**). These values remained remarkably consistent throughout the simulations, indicating that the overall hydrogen-bond network of PKN1 is preserved upon ligand binding. Notably, the PKN1-IMPHY012968 complex exhibited the highest average number of intramolecular hydrogen bonds (154), suggesting a modest internal cohesion and structural rigidity enhancement. simulations.

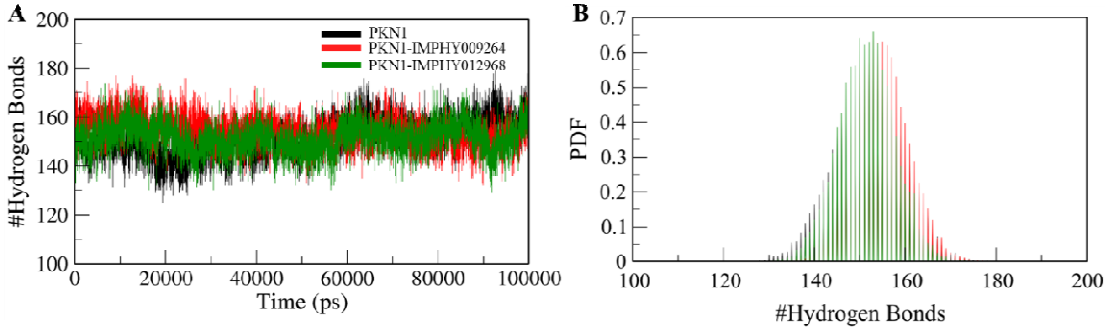


Figure 7: (A) Dynamics of intramolecular hydrogen bonds formed between free PKN1 and in complex with IMPHY0010989, IMPHY012968. (B) Probability density function (PDF).

IV. Principal Component Analysis

Principal component analysis evaluated protein and protein ligand complex conformational changes and collective motions. PCA was employed to explore the dominant motions of alpha carbon atoms in free PKN1 and its complexes with IMPHY012968 and IMPHY009264 based on the 100 ns molecular dynamics trajectories (**Figure 8A-C**). Figure X shows the projection of each simulation onto the first two eigenvectors EV1 and EV2, which together capture the majority of structural variance.

The free PKN1 trajectory in black populates three distinct sub-regions in the EV1 EV2 space, indicating an intrinsic flexibility that allows the protein to sample multiple conformational basins. Upon binding IMPHY012968, shown in red, PKN1 explores a similarly broad region, albeit slightly shifted along EV1 and EV2, suggesting that this ligand induces new collective motions without greatly restricting the protein's dynamics. In contrast, the PKN1 IMPHY009264 complex in green occupies a noticeably more confined subspace, with a tighter cluster of points in both EV dimensions.

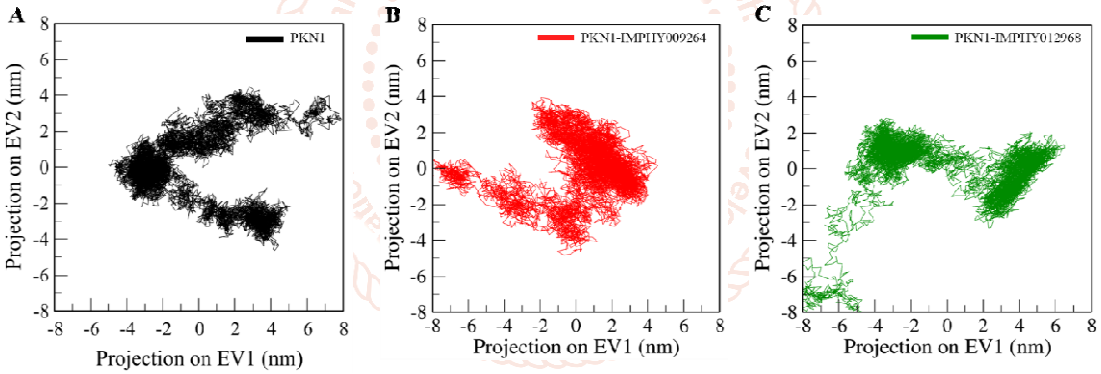


Figure 8: Conformational subspace in the principal component analysis of (A) PKN1, (B) IMPHY012968, (C) IMPHY009264.

CONCLUSION

The molecular dynamics simulations conducted over 100 ns have demonstrated that both IMPPAT-based compounds, IMPHY012968 and IMPHY009264, effectively stabilize the PKN1 structure relative to the control compound. RMSD and RMSF analyses revealed that the protein backbone and individual residues fluctuate minimally when bound to the zinc ligands, closely mirroring the behavior of the apo form. Radius of gyration and solvent accessible surface area measurements further confirmed that the IMPHY009264 complex adopts the most compact conformation with the least exposed surface. Intramolecular hydrogen bond counts remained consistently high across all systems, with a slight increase in the IMPHY012968 complex suggesting enhanced internal cohesion. Intermolecular hydrogen bond analysis showed that each ligand maintains two stable protein interactions, anchoring them in their binding pockets and contributing to overall complex integrity. Principal component analysis underscored these findings by demonstrating that binding of ligands significantly narrows the conformational landscape, reducing the accessible motion to the fewest substates. Collectively, these complementary metrics illustrate that IMPHY012968 and IMPHY009264 engage PKN1 in a manner that preserves its native fold, minimizes unwanted flexibility, and confines the protein to its most stable conformational basins. These stabilizing effects, coupled with favorable docking and binding free energy profiles, nominate these IMPPAT compounds as promising lead candidates for further development against PKN1-linked pathologies.

REFERENCES

[1] Mukai H. The structure and function of PKN, a protein kinase having a catalytic domain homologous to that of PKC. J Biochem. 2003; 133(1): 17-27.

[2] Sophocleous G, Owen D, Mott HR. The structure and function of protein kinase C-related kinases (PRKs). Biochem Soc Trans. 2021; 49(1): 217-35.

[3] Fabbro D, Cowan-Jacob SW, Moebitz H. Ten things you should know about protein kinases: IUPHAR Review 14. Br J Pharmacol. 2015; 172(11): 2675-700.

[4] Lachmann S, Jevons A, De Rycker M, Casamassima A, Radtke S, Collazos A, Parker PJ. Regulatory domain selectivity in the cell-type specific PKN-dependence of cell migration. PLoS One. 2011; 6(7): e21732.

[5] Quetier I, Marshall JJ, Spencer-Dene B, Lachmann S, Casamassima A, Franco C, et al. Knockout of the PKN family of Rho effector kinases reveals a non-redundant role for PKN2 in developmental mesoderm expansion. Cell Rep. 2016; 14(3): 440-8.

[6] Kornev AP, Haste NM, Taylor SS, Ten Eyck LF. Surface comparison of active and inactive protein kinases identifies a conserved activation mechanism. Proc Natl Acad Sci U S A. 2006; 103(47): 17783-8.

[7] Kornev AP, Taylor SS, Ten Eyck LF. A helix scaffold for the assembly of active protein kinases. Proc Natl Acad Sci U S A. 2008; 105(38): 14377-82.

[8] Meharena HS, Chang P, Keshwani MM, Oruganty K, Nene AK, Kannan N, et al. Deciphering the structural basis of eukaryotic protein kinase regulation. PLoS Biol. 2013; 11(10): e1001680.

[9] Modi V, Dunbrack RL Jr. Defining a new nomenclature for the structures of active and inactive kinases. Proc Natl Acad Sci U S A. 2019; 116(14): 6818-27.

[10] Modi V, Dunbrack RL Jr. Kincore: a web resource for structural classification of protein kinases and their inhibitors. Nucleic Acids Res. 2022; 50(D1): D654-64.

[11] Moebitz H. The ABC of protein kinase conformations. Biochim Biophys Acta Proteins Proteom. 2015; 1854(10): 1555-66.

[12] Noble ME, Endicott JA, Johnson LN. Protein kinase inhibitors: insights into drug design from structure. Science. 2004; 303(5665): 1800-5.

[13] Gógl G, Kornev AP, Reményi A, Taylor SS. Disordered protein kinase regions in regulation of kinase domain cores. Trends Biochem Sci. 2019; 44(4): 300-11.

[14] Kanev GK, de Graaf C, de Esch IJ, Leurs R, Würdinger T, Westerman BA, Kooistra AJ. The landscape of atypical and eukaryotic protein kinases. Trends Pharmacol Sci. 2019; 40(11): 818-32.

[15] Mukai H, Toshimori M, Shibata H, Kitagawa M, Shimakawa M, Miyahara M, et al. PKN associates and phosphorylates the head-rod domain of neurofilament protein. J Biol Chem. 1996; 271(16): 9816-22.

[16] Collard JF, Côté F, Julien JP. Defective axonal transport in a transgenic mouse model of amyotrophic lateral sclerosis. Nature. 1995; 375(6526): 61-4.

[17] Williamson TL, Cleveland DW. Slowing of axonal transport is a very early event in the toxicity of ALS-linked SOD1 mutants to motor neurons. Nat Neurosci. 1999; 2(1): 50-6.

[18] Xiao S, McLean J, Robertson J. Neuronal intermediate filaments and ALS: a new look at an old question. Biochim Biophys Acta Mol Basis Dis. 2006; 1762(11-12): 1001-12.

[19] James RG, Bosch KA, Kulikauskas RM, Yang PT, Robin NC, Toroni RA, et al. Protein kinase PKN1 represses Wnt/β-catenin signaling in human melanoma cells. J Biol Chem. 2013; 288(48): 34658-70.

[20] Kato T Jr, Gotoh Y, Hoffmann A, Ono Y. Negative regulation of constitutive NF-κB and JNK signaling by PKN1-mediated phosphorylation of TRAF1. Genes Cells. 2008; 13(5): 509-20.

[21] Standaert M, Bandyopadhyay G, Galloway L, Ono Y, Mukai H, Farese R. Comparative effects of GTPγS and insulin on the activation of Rho, phosphatidylinositol 3-kinase, and protein kinase N in rat adipocytes: relationship to glucose transport. J Biol Chem. 1998; 273(13): 7470-7.

[22] Dong LQ, Landa LR, Wick MJ, Zhu L, Mukai H, Ono Y, et al. Phosphorylation of protein kinase N by phosphoinositide-dependent protein kinase-1 mediates insulin signals to the

actin cytoskeleton. Proc Natl Acad Sci U S A. 2000; 97(10): 5089-94.

[23] Herrerías-González F, Yeramian A, Baena-Fustegueras JA, Bueno M, Fleitas C, de la Fuente M, et al. PKN1 kinase: a key player in adipocyte differentiation and glucose metabolism. Nutrients. 2023; 15(10): 2414.

[24] Chen F, Moran JT, Zhang Y, Ates KM, Yu D, Schrader LA, et al. The transcription factor NeuroD2 coordinates synaptic innervation and cell intrinsic properties to control excitability of cortical pyramidal neurons. J Physiol. 2016; 594(13): 3729-44.

[25] Ince-Dunn G, Hall BJ, Hu SC, Ripley B, Huganir RL, Olson JM, et al. Regulation of thalamocortical patterning and synaptic maturation by NeuroD2. Neuron. 2006; 49(5): 683-95.

[26] Olson JM, Asakura A, Snider L, Hawkes R, Strand A, Stoeck J, et al. NeuroD2 is necessary for development and survival of central nervous system neurons. Dev Biol. 2001; 234(1): 174-87.

[27] Wilke SA, Hall BJ, Antonios JK, DeNardo LA, Otto S, Yuan B, et al. NeuroD2 regulates the development of hippocampal mossy fiber synapses. Neural Dev. 2012; 7:1-14.

[28] Safari MS, Obexer D, Baier-Bitterlich G, Zur Nedden S. PKN1 is a novel regulator of hippocampal GluA1 levels. Front Synaptic Neurosci. 2021; 13:640495.

[29] Jilg CA, Ketscher A, Metzger E, Hummel B, Willmann D, Rüsseler V, et al. PRK1/PKN1 controls migration and metastasis of androgen-independent prostate cancer cells. Oncotarget. 2014; 5(24): 12646-64.

[30] Wang X, Ge Y, Shi M, Dai H, Liu W, Wang P. Protein kinase N1 promotes proliferation and invasion of liver cancer. Exp Ther Med. 2021; 21(6): 651.

[31] Galgano MT, Conaway M, Spencer AM, Paschal BM, Frierson HF Jr. PRK1 distribution in normal tissues and carcinomas: overexpression and activation in ovarian serous carcinoma. Hum Pathol. 2009; 40(10): 1434-40.

[32] Attarha S, Andersson S, Mints M, Souchelnytskyi S. Individualised proteome profiling of human endometrial tumours improves detection of new prognostic markers. Br J Cancer. 2013; 109(3): 704-13.

[33] Attarha S, Saini RKR, Andersson S, Mints M, Souchelnytskyi S. PKN1 modulates TGFβ and EGF signaling in HEC-1-A endometrial cancer cell line. Onco Targets Ther. 2014; 7:1397-408.

[34] Safari MS, Woerl P, Garmsiri C, Weber D, Kwiatkowski M, Hotze M, et al. Glucose-1,6-bisphosphate: a new gatekeeper of cerebral mitochondrial pyruvate uptake. Mol Metab. 2024; 88:102018.

[35] Francois AA, Obasanjo-Blackshire K, Clark JE, Boguslavskyi A, Holt MR, Parker PJ, et al. Loss of Protein Kinase Novel 1 (PKN1) is associated with mild systolic and diastolic contractile dysfunction, increased phospholamban Thr17 phosphorylation, and exacerbated ischaemia-reperfusion injury. Cardiovasc Res. 2018; 114(1): 138-57.

[36] Yuan Q, Ren C, Xu W, Petri B, Zhang J, Zhang Y, et al. PKN1 directs polarized RAB21 vesicle trafficking via RPH3A and is important for neutrophil adhesion and ischemia-reperfusion injury. Cell Rep. 2017; 19(12): 2586-97.